ELSEVIER

Journal of Alloys and Compounds 434–435 (2007) 115–118

Journal of ALLOYS AND COMPOUNDS

www.elsevier.com/locate/jallcom

Influence of microalloying on glass formation and crystallization

K.F. Kelton *

Department of Physics and Center for Materials Innovation, Campus Box 1105, Washington University, St. Louis, MO 63130, USA

Available online 20 September 2006

Abstract

The influence of extremely small amounts of early transition metals on glass formation has recently been demonstrated in Al–Y–Fe alloys. Although rapidly quenched samples of $Al_{88}Y_7Fe_5$ have X-ray diffraction patterns that are typical of amorphous metallic alloys, the isothermal differential scanning calorimetry (DSC) data do not show the expected nucleation and growth peak associated with the formation of nano-sized grains of α-Al. Samples prepared with Ti ($Al_{88-x}Y_7Fe_5Ti_x$ with $x = 0.5$, 1, 2) transform at higher temperatures and show the DSC isothermal peak expected for glass crystallization. It is often claimed that the absence of an isothermal DSC peak indicates that the samples are not glasses, but are actually fully transformed nanocrystal composites, with the monotonic DSC trace indicating a coarsening of the nanocrystals. However, calculations presented here show that it could also be explained by diffusion-controlled nucleation and growth, with a high nucleation rate due to a change in the local structure of the glass.

Keywords: Amorphous materials; Metals; Liquid quenching; Nanostructure; Thermal analysis

1. Introduction

Many Al-, Fe-, Mg- and Zr-based metallic glasses crystallize to an amorphous/nanocrystal composite (nano-composite). Often these nano-composites are more interesting and have greater technological potential than their glass precursors [1–2]. The high grain densities (10^{20}–$10^{23}/m^3$) and nanometer-sized grains indicate an extremely high nucleation rate and a low growth velocity. Grain growth is typically initially rapid, but abruptly slows down when the grain size exceeds a few nanometers; there is also little temperature dependence of the final grain sizes [3].

The substitution of small amounts of Ti for Al improves glass formation and stability in Al–Y–Fe alloys that form nano-grains of α-Al during primary crystallization [4]. The Ti appears to alter the local structure of the glass, leading to a higher barrier for the nucleation of α-Al. Isothermal differential scanning calorimetry (DSC) curves for the Al–Y–Fe glasses made without Ti show a monotonically decreasing signal that is commonly interpreted as coarsening of a completely transformed nano-composite [4–6]. Our recent calculations, however, demonstrate that this could also indicate diffusion-limited growth on a high density of quenched-in nuclei. These points are reviewed briefly here.

2. Al–Y–Fe–Ti—an example of microalloying

Often glass formation and crystallization can be profoundly influenced by the addition of small amounts of particular elements (microalloying). In the Zr-based glasses, for example, it is well known that crystallization to the icosahedral quasicrystal phase is enhanced by the addition of O [7,8], noble elements such as Ag, Au, Pd and Pt [9] and the transition metals Nb, Ta, V [10] and Ti [11,12]. Ag, Au, Pd and Pt have strong negative heats of mixing with Zr, but interact only weakly with Ni or Cu [13], suggesting that strongly bound icosahedral clusters may form around the transition metals, giving rise to strong icosahedral short-range order in the liquid/glass. These arguments build upon Frank's hypothesis that the structures of liquid metals are dominated by icosahedral order [14]. We recently confirmed Frank's hypothesis in a Ti–Zr–Ni liquid, correlating an increasing icosahedral order (ISRO) in the undercooled liquid with a decreasing nucleation barrier for the icosahedral phase [15]. If the microadditions enhance the ISRO in the liquid, nucleation will become more difficult during the quench, enhancing glass formation. Further, the inherited icosahedral order in the resulting glass will favor the primary nucleation of the i-phase during devitrification, as observed.

* Tel.: +1 314 935 6229; fax: +1 314 935 6219.
E-mail address: kfk@wuphys.wustl.edu.

0925-8388/$ – see front matter © 2006 Elsevier B.V. All rights reserved.
doi:10.1016/j.jallcom.2006.08.138

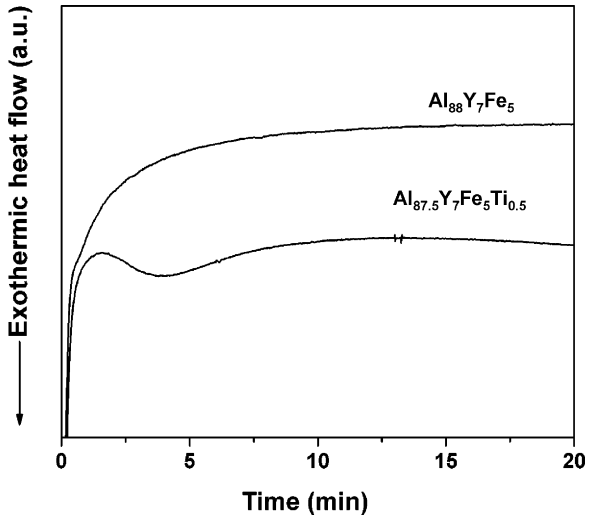

Fig. 1. DSC traces for isothermal annealing for Al–Y–Fe and Al–Y–Fe–Ti samples, showing the expected nucleation and growth peak in the sample containing Ti and a monotonic decrease in the heat evolved for the sample without Ti (data taken from Ref. [4]).

However, microadditions need not lead to only ISRO to influence glass formation and crystallization. They must only enhance a short-range order in the liquid or glass that is incompatible with that of the crystallizing phase. In 3d-transition metals, for example, we recently demonstrated that there can exist a competition between packing constraints that favor ISRO and bonding properties that may favor a different short-range order, often leading to a distortion in the ISRO [16]. The nucleation barrier for crystal phases is little affected by the degree of perfection of the ISRO, however.

In Al–Y–Fe alloys it is likely that the microaddition enhances a different type of order in the liquid and glass. Rapidly quenched ribbons of $Al_{88}Y_7Fe_5$ show glass-like X-ray and transmission electron microscopy (TEM) diffraction patterns, no evidence for crystal diffraction peaks or precipitates in TEM bright-field images, and an exothermic peak in nonisothermal DSC measurements [17]. However, the isothermal DSC data show a monotonic decrease in the rate at which heat is evolved with annealing time (Fig. 1). This is typically taken to indicate grain coarsening [6], suggesting that the rapidly quenched sample is not a glass, but a completely transformed nano-composite, although as will be discussed in Section 3 this is not the only possible interpretation. The substitution of some of the Al by a small amount of Ti dramatically improves glass formation and stability [4]. The isothermal DSC curves from rapidly quenched $Al_{87.5}Y_7Fe_5Ti_{0.5}$ samples contain a peak that is characteristic of nucleation and growth during glass crystallization (Fig. 1).

Studies of $Al_{87.5}Y_7Fe_5Ti_{0.5}$ samples in which oxygen was deliberately introduced by substituting Fe_2O_3 for a portion of the iron demonstrated that the Ti was not acting simply as an oxygen scavenger [4]. When the oxygen concentration exceeded >0.5 at.%, monotonic DSC curves were always obtained, irrespective of the amount of Ti present. Further, the temperature of onset of primary crystallization to α-Al was unaltered by the oxygen concentration, although it did suppress the formation of a metastable phase that occurred near 340 °C in samples containing no oxygen, replacing it by a bcc phase ($a = 0.317$ nm) that formed at a slightly higher temperature, near 370 °C. In contrast, the introduction of Ti moved the onset of α-Al crystallization approximately 30 °C higher and enhanced the formation of the metastable phase. Transmission electron microscopy studies showed that a higher annealing temperature was required for $Al_{87.5}Y_7Fe_5Ti_{0.5}$ than for $Al_{88}Y_7Fe_5$ to produce a comparable density of α-Al crystals. Larger crystals were produced at the higher temperature, however, demonstrating that the Ti primarily influenced the nucleation barrier instead of the growth rate, likely by changing the local structure of the glass. Recent high-energy X-ray synchrotron studies [18] support this conclusion.

3. Nucleation and long-range diffusion

The primary crystallization of the Al–Y–Fe–Ti glasses is governed by the diffusion of Y and Fe away from the nucleating and growing α-Al grains. The large difference in the diffusion rates of the alloy components causes an enrichment of the rare earth near the growing crystallites [19], slowing Al diffusion and hence the growth rate. Since the classical theory of nucleation is inherently an interface-limited theory [20], it is not applicable when the interfacial attachment rates are competitive with the atomic transport rates to the regions of the developing clusters. In such cases, these two stochastic fluxes become coupled. Following an approach first suggested by Russell [21], this may be treated to lowest order by focusing attention on three regions: the cluster, the immediate neighborhood around the cluster (the shell region) and the parent phase [22,23]. In this model, the flux between the shell and the parent phase is coupled with that between the shell and the cluster. The cluster evolution underlying time-dependent nucleation is determined by solving numerically a system of coupled differential equations,

$$\begin{aligned}\frac{\partial N(n,\rho)}{\partial t} &= \alpha(n,\rho-1)\times N(n,\rho-1) - [\alpha(n,\rho)+\beta(n,\rho)] \\ &\quad \times N(n,\rho) + \beta(n,\rho+1)\times N(n,\rho+1) \\ &\quad + k^{+}(n-1,\rho+1)\times N(n-1,\rho+1) \\ &\quad + k^{-}(n+1,\rho-1)\times N(n+1,\rho-1) \\ &\quad - [k^{+}(n,\rho)+k^{-}(n,\rho)]\times N(n,\rho), \end{aligned} \tag{1}$$

where $N(n,\rho)$ is the density of clusters containing n solute atoms (here Al), with ρ solute atoms in the shell region immediately outside the cluster interface; α and β represent the rates at which atoms arrive and leave the cluster shell, respectively, and $k^{\pm}$ represent the interfacial attachment (+) and detachment (−) rates. Predictions from the coupled-flux model approach those from the classical theory in the limit of high concentration and high diffusion rates in the parent phase [22,23].

By dividing the time of an isothermal anneal into a series of short anneals, allowing the cluster evolution to proceed according to Eq. (1) for each anneal, the volume fraction transformed was computed as a function of time, $x(t)$. Implicit numerical

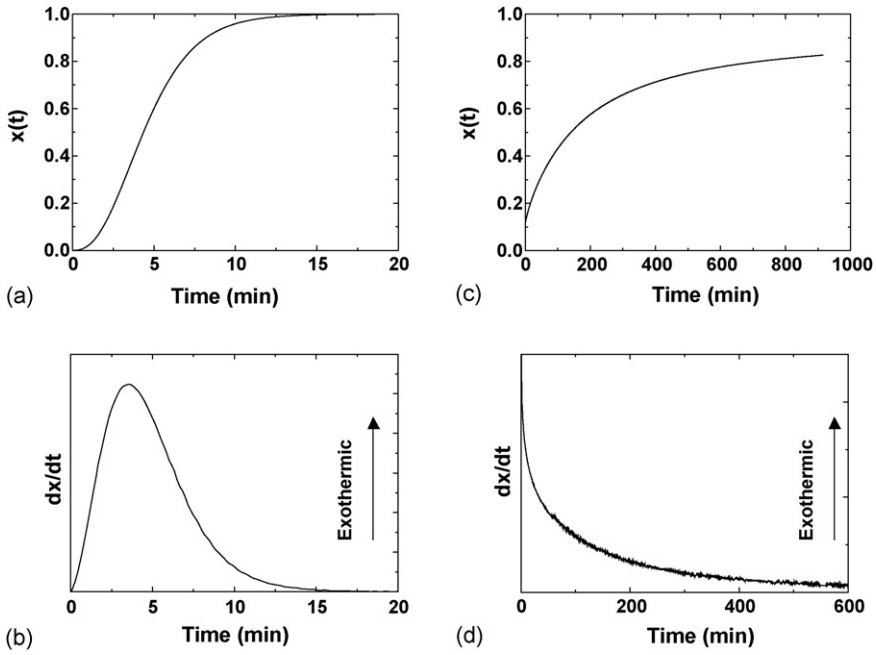

Fig. 2. Calculations made using effective parameters for the diffusion coefficient (10^{17} m^2/s) and driving free energy (15.3 kT). (a) Computed volume fraction transformed, $x(t)$ and (b) dx/dt ($\propto$dH/dt) for an interfacial free energy yielding 10^{23}/m^3 nuclei ($\sigma = 0.68$ J/m^2) (c) $x(t)$ and (d) dx/dt ($\propto$dH/dt) for $\sigma = 0.38$ J/m^2, yielding 10^{26}/m^3 nuclei. When comparing these results for dx/dt with those in Fig. 1, note that the signs of exothermic heat are different in the two figures.

methods were used to compute the cluster evolution (see Ref. [22] for details). The growth of clusters that evolved past the upper limit of the cluster distribution (typically 10 times the critical size for nucleation) was computed using an expression for the diffusion-limited, size-dependent growth rate [22], which for a pure solute precipitate is approximately

$$\frac{dn}{dt} \approx (4\pi)^{2/3}(3n\bar{v})^{1/3}c_{\infty}(t)D \quad (2)$$

where D is the diffusion coefficient of the solute atom in the initial phase, $\bar{v}$ the atomic volume and $c_{\infty}(t)$ is the time-dependent concentration of the initial phase, far from the cluster.

Effective parameters were chosen to probe the influence of the nuclei density on the transformation kinetics; the results are compiled in Fig. 2. It should be emphasized that these parameters were not chosen to make a quantitative comparison with the isothermal DSC experimental data, but to investigate whether it was possible to obtain a monotonic DSC curve for glass crystallization instead of nanocrystal coarsening. With the chosen parameters, the expected sigmoidal curve for the volume fraction transformed as a function of time, $x(t)$, is observed, even for a large number of nuclei ($\approx 10^{23}$/m^3) (Fig. 2a). A transformation peak is observed in dH/dt (the signal in an isothermal DSC experiment), which is proportional to dx/dt (Fig. 2b). If the nuclei density is increased by three orders of magnitude ($\approx 10^{26}$/m^3), however, soft-impingement becomes severe in the earliest stages of the transformation, causing a sharp rise in $x(t)$ for small times, followed by a radically slower transformation rate (Fig. 2c). Correspondingly, a peak in dx/dt occurs at very short times and is followed by a monotonically decreasing rate of change (Fig. 2d). This latter behavior follows for a smaller number of growth centers if the diffusion coefficient of the solute to the growing crystals decreases with the fraction transformed, as expected for the precipitation of α-Al with the rejection of Y to the glass. Fig. 2b is similar to the experimentally observed curves for $Al_{87.5}Y_5Fe_7Ti_{0.5}$ (Fig. 1), and corresponds to the expected nucleation and growth behavior. Fig. 2d is like the experimental data for $Al_{88}Y_5Fe_7$ (Fig. 1), which was previously attributed to coarsening [4].

The density of α-Al quenched-in nuclei or nanocrystals in $Al_{88}Y_7Fe_5$ is large ($\geq 10^{21}$/m^3). For these to form during the quench would require an extraordinarily high steady-state nucleation rate, particularly given that the nucleation rate is strongly suppressed during quenching due to transient nucleation [24]. It is difficult to understand how such a high nucleation rate can arise within the classical theory of nucleation. The coupled-flux model predicts that shell region for clusters of α-Al that are smaller than the critical size will be enriched, rather than depleted, in Al; this has recently been confirmed by a kinetic Monte Carlo ising lattice gas calculation [25]. Due to transient nucleation, the cluster density and shell concentration from a high temperature, with a correspondingly large critical size, will be frozen in during the quench. Upon annealing the glass at a lower temperature, where the critical size is smaller, a large population of clusters will grow quickly, consuming the excess Al. The growth rate will then abruptly decrease since long-range diffusion to the cluster will be required. Within this model a high density of nano-size crystals arises naturally [26].

4. Conclusions

The addition of small concentrations of Ti (≈0.5 at.%) to $Al_{88}Y_7Fe_5$ glasses dramatically improves glass formation and stability, likely by modifying the local structure of the glass and

increasing the nucleation barrier for α-Al and likely other competing intermetallic phases. A realistic calculation based on the coupled-flux model for nucleation, which fully incorporates the effects of diffusion in both nucleation and growth, demonstrates that a monotonic decreasing signal, which is generally taken as an indication of the coarsening of a nanocrystal material could also be a sign of diffusion-limited growth of a very high density of nuclei. A simple DSC isothermal test, then, is insufficient to decide between a glass and a completely transformed amorphous/nanocrystal composite when the nucleation rate is high and soft-impingement is dominant.

Acknowledgements

This work was supported by the National Science Foundation under grant DMR 03-07410 and the US Air Force Office of Scientific Research Scientific Research under contract FA9550-05-1-0110.

References

[1] A. Inoue, Prog. Mater. Sci. 43 (1998) 365.
[2] A.L. Greer, Mater. Sci. Eng. A 304–306 (2001) 68.
[3] M. Calin, U. Koester, Mater. Sci. Forum 269-272 (1998) 749.
[4] L.Q. Xing, A. Mukhopadhyay, W.E. Buhro, K.F. Kelton, Philos. Mag. Lett. 84 (2004) 293.
[5] L.C. Chen, F. Spaepen, J. Appl. Phys. 69 (1991) 679.
[6] L.C. Chen, F. Spaepen, Mater. Sci. Eng. A A133 (1991) 342.
[7] J. Eckert, N. Mattern, M. Zinkevitch, M. Seidel, Mater. Trans. JIM 39 (1998) 623.
[8] B.S. Murty, D.H. Ping, Mater. Sci. Eng. A A304–A306 (2001) 706.
[9] A. Inoue, T. Zhang, J. Saida, M. Matsushita, M. Chen, T. Sakurai, Mater. Trans. JIM 40 (1999) 1181.
[10] J. Saida, J. Phys. Condens. Matter 13 (2001) L73.
[11] L.Q. Xing, T.C. Hufnagel, J. Eckert, W. Loser, L. Schultz, Appl. Phys. Lett. 77 (2000) 1970.
[12] L.Q. Xing, Y.T. Shen, K.F. Kelton, Appl. Phys. Lett. 81 (2002) 3371.
[13] A.K. Niessen, F.R. de Boer, S. Boom, P.F. de Chatel, W.C.M. Mattens, A.R. Miedema, CALPHAD: Comput. Coupling Phase Diagrams Thermochem. 7 (1983) 51.
[14] F.C. Frank, Proc. R. Soc. Lond. 215A (1952) 43.
[15] K.F. Kelton, G.W. Lee, A.K. Gangopadhyay, R.W. Hyers, T. Rathz, J. Rogers, M.B. Robinson, D. Robinson, Phys. Rev. Lett. 90 (2003) 195504.
[16] G.W. Lee, A.K. Gangopadhyay, K.F. Kelton, R.W. Hyers, T.J. Rathz, J.R. Rogers, D. Robinson, Phys. Rev. Lett. 93 (2004) 37802.
[17] D.R. Allen, J.C. Foley, J.H. Perepezko, Acta Mater. 46 (1998) 431.
[18] T.H. Kim, A.K. Gangopadhyay, A.I. Goldman, K.F. Kelton, private communication.
[19] K. Hono, Y. Zhang, A. Inoue, T. Sakurai, Mater. Sci. Eng. A226–228 (1997) 498.
[20] K.F. Kelton, in: H. Ehrenreich, D. Turnbull (Eds.), Solid State Physics, Academic Press, Boston, 1991, p. 75.
[21] K.C. Russell, Acta Metall. 16 (1968) 761.
[22] K.F. Kelton, Acta Mater. 48 (2000) 1967.
[23] K.F. Kelton, J. Non-Cryst. Solids 274 (2000) 147.
[24] K.F. Kelton, A.L. Greer, J. Non-Cryst. Solids 79 (1986) 295.
[25] J. Diao, R. Salazar, K.F. Kelton, L.D. Gelb (private communication).
[26] K.F. Kelton, Philos. Mag. Lett. 77 (1998) 337.